Differential impacts of contact tracing and lockdowns on outbreak size in COVID-19 model applied to China

Cameron J. Browne,[1*] Hayriye Gulbudak,[1] Joshua C. Macdonald[1]

[1]Department of Mathematics, University of Louisiana at Lafayette,
[*]To whom correspondence should be addressed; E-mail: cambrowne@louisiana.edu.

Rapid growth of the COVID-19 epidemic in China induced extensive efforts of contact tracing and social-distancing/lockdowns, which quickly contained the outbreak and has been replicated to varying degrees around the world. We construct a novel infectious disease model incorporating these distinct quarantine measures (contact tracing and self-quarantine) as reactionary interventions dependent on current infection levels. Derivation of the final outbreak size leads to a simple inverse proportionality relationship with self-quarantine rate, revealing a fundamental principle of exponentially increasing cumulative cases when delaying mass quarantine or lockdown measures beyond a critical time period. In contrast, contact tracing results in a proportional reduction in reproduction number, flattening the epidemic curve but only having sizable impact on final size when a large proportion of contacts are "perfectly" traced. We fit the mathematical model to data from China on reported cases and quarantined contacts, finding that lockdowns had an overwhelming influence on outbreak size and duration, whereas contact tracing played a role in reducing peak number of infected. Sensitivity analysis and simulations under different

re-opening scenarios illustrate the differential effects that responsive contact tracing and lockdowns can have on current and second wave outbreaks.

1 Introduction

The current COVID-19 pandemic began in Wuhan, China, where infections grew rapidly and spread throughout the country in late December 2019 and January 2020. In order to contain the virus, drastic measures, such as travel restrictions alongside extensive lockdowns and contact tracing efforts, were implemented. The overall success of these control strategies in suppressing the outbreak in China has been recognized in several studies (*1, 2*). An important question is which intervention had the largest impact, or in more detail, quantifying the effect of each intervention on case reduction. The problem is relevant not only for retrospective analysis, as all countries including China face the task of controlling ongoing or possible second wave outbreaks of COVID-19.

The strategies currently available for the fight against COVID-19 are often classified as non-pharamacuetical interventions (NPIs), since consensus vaccines or treatments have not been found to date. The effectiveness and aims of NPIs may vary by country and type of intervention. While the goal of large-scale lockdowns and social distancing is often characterized as "flattening the curve", whereas successful contact tracing may suppress outbreaks, a more nuanced picture of their potential impact on epidemic trajectories is necessary. A few studies have quantified impact of travel restrictions (*3, 4*) and lockdowns inducing large-scale changes in contact patterns or depletion of susceptible individuals (*5, 6*), showing the efficacy of these interventions in China. Yet, the precise qualitative and quantitative effect of brute force interventions such as lockdowns (or widespread social distancing), versus the more targeted strategy of contact tracing, on the outbreak shape is less explored.

Traditionally the influence of control strategies on outbreaks has been theoretically inves-

tigated in compartmental ordinary differential equation models of the susceptible-infected-recovered (SIR) type. Analysis yields the herd immunity (or critical vaccination) threshold for suppressing an outbreak by proportionally reducing the reproduction number, $\mathcal{R}_0$, below one, along with a nonlinear relationship between $\mathcal{R}_0$ and final outbreak size when $\mathcal{R}_0$ is above one. Furthermore, inference of parameters by fitting the model to data can help to determine the effect of interventions. However both the analytical and parameter estimation approaches are challenged by the dynamic nature of control strategies as public health authorities and individuals react to an evolving outbreak.

While the early phase of COVID-19 can be characterized by exponential growth, case saturation occurred much earlier than would be predicted by the basic SIR model due to the comprehensive control measures that have been deployed. In particular, stringent lockdown with broad (self- and contact tracing) quarantine interventions reduced the pool of susceptible individuals, effective contact rate and secondary transmissions. Several models have utilized time-dependent transmission or isolation rates to capture the dynamics (*3, 7*), and recent work has also considered removal of susceptible individuals at a constant rate (*6*). Here we develop a generalized SIR-type model incorporating a total (government mandated and individual) social distancing rate, along with contact tracing, both *depending on overall infection rate*, in order to fit an observed reactionary public health system and derive novel formulae for outbreak size.

In order to quantify the impacts of contact tracing and comprehensive social distancing (or lockdowns), we simultaneously utilize case and quarantined contact data from China to estimate parameters in our model. Furthermore, through computational and theoretical analysis of the model, we can explore the sensitivity of distinct epidemic measures (e.g. outbreak size, peak number of infected, timing and extent of social distancing) to interpretable control parameters. These investigations allow us to dissect how combinations of NPIs, such as contact tracing and lockdowns, may influence sequential outbreaks through loosening and tightening of

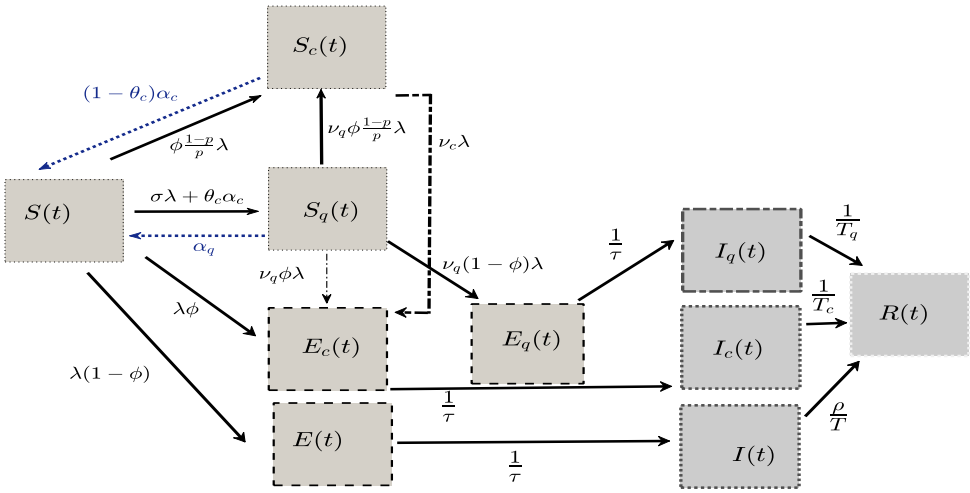

Figure 1: *Full compartmental model of COVID-19 with reactive contact tracing and self-quarantine.* We extend the basic SEIR model describing infection of susceptibles (S) at rate β, pre-infectious compartment (E) of average length τ and infectious compartment (I) of avg. period T. Contact tracing is incorporated by tracking a proportion ϕ of reported case contacts whom are either susceptible (S_c) with reduction in susceptibility ν_c for average time of $1/\alpha_c$, or infected (E_c, I_c) and have reduced reproduction number $\beta_c T_c$. Self-quarantine (social distancing) of susceptibles (S_q) is implemented at rate σ proportional to "force of infection" $\lambda = \beta I + \beta_q I_q + \beta_c I_c$ with reduction in susceptibility ν_q for average time of $1/\alpha_q$, and can be infected (E_q, I_q) with reduced reproduction number $\beta_q T_q$. In the simplified system (1), we consider "indefinite" self-quarantine ($\alpha_q = 0$) where contact traced susceptibles always transition ($\theta_c = 1$), along with perfect contact tracing and self-quarantine ($\nu_c = \nu_q = \beta_c = \beta_q = 0$).

control measures. The emergent picture is of distinct qualitative impacts of contact tracing and lockdowns on the outbreak, variable in scope and timing, and dependent on underlying disease parameters. A better understanding of these differential effects can help shape or suppress the epidemic curve of COVID-19 in a sustainable and acceptable manner to societies.

2 Model with Social Distancing and Contact Tracing

We formulate a SEIR model (Fig.1 and generalized equations are given in Supplementary), which modifies a detailed differential equation system of contact tracing during outbreaks (*8*). The model variables include: susceptible (S), exposed (E) and infectious (I) individuals; social-distanced (or self-quarantined) susceptible (S_q), exposed (E_q) and infectious (I_q) individuals; contact traced susceptible (S_c), exposed (E_c), and infectious (I_c) individuals; and the decou-

pled compartments of (safely) isolated reported cases (R) with a subset of currently quarantined contact-traced cases (R_c). The full system of equations, along with a table of variables and parameters, are given in the Supplementary. Here we highlight a few key features of the model. Parameters β, β_c, and β_q represent transmission rates of reported un-quarantined, contact traced quarantined and social-distanced infected individuals, respectively, where β_c and β_q reflect reductions in transmission due to contact tracing and social distancing which are generally imperfect (e.g. tracing individual after they become infectious, looseness in following stay-at-home orders). A critical control parameter is the total rate of susceptible transition to (contact traced or self-) quarantine state, $\psi\lambda S$, with $\psi = \frac{1-p}{p}\phi + \sigma$, depending on force of infection $\lambda = \beta I + \beta_q I_q + \beta_c I_c$, the proportion of contacts traced ϕ, the probability of transmission upon contact p and the self-quarantine (social distancing or lockdown) rate σ. The dependence on force of infection reflects mechanism of contact tracing (*8*), along with the responsive nature of broader social distancing/quarantine measures to current transmission. Other important parameters include α_q, the rate of return to susceptible from social distancing, and ν_q the susceptibility of social-distanced individuals measuring the looseness of the social distancing measures.

A simplified version of the model assuming *perfect indefinite* quarantine and *perfect* contact tracing is given by the following system:

$$\begin{aligned} S' &= -\left(1+\psi\right)\beta SI, \quad E' = \left(1-\phi\right)\beta SI - \frac{1}{\tau}E, \\ I' &= \frac{1}{\tau}E - \frac{1}{T}I, \quad R' = \frac{1}{T}I + \frac{1}{T_c}I_c + \frac{1}{T_q}I_q, \end{aligned} \tag{1}$$

where R is decoupled, and the additional decoupled compartments of self-quarantined and contact traced (fit to data) are detailed in the Supplementary. In Section 4, we fit both the simplified model and full model above to total case and quarantined contact data of China.

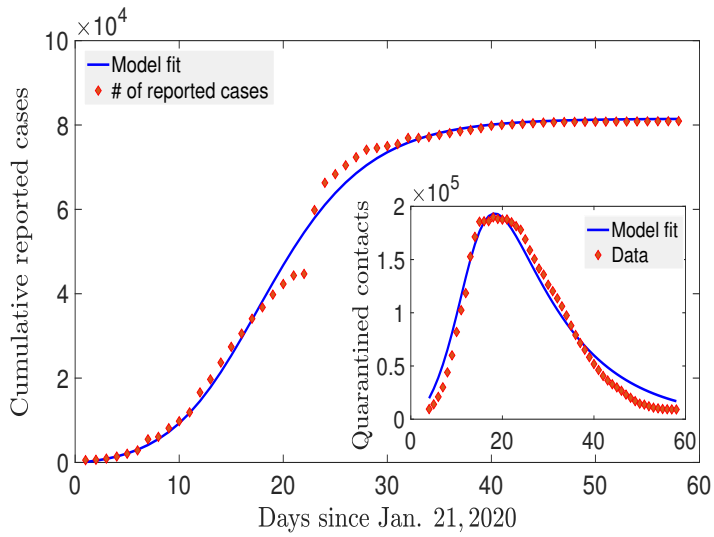

Figure 2: *Model recapitulates case and contact tracing data, estimates large rate of self-quarantine (via lockdown) rapidly contains outbreak.* (a) Cumulative reported cases and daily number of quarantined contacts (inserted figure) simultaneously fit to model (1). (b) The corresponding daily reported cases in model with data and inferred subset of contact traced infected. (c) Average and daily impact of contact tracing on $\mathcal{R}_e$ from estimated parameters utilizing statistical method based on generation time distribution. Observe the reduction in $\mathcal{R}_e$ with or without contact tracing due to social distancing/lockdowns is the major factor to rapidly contain the outbreak.

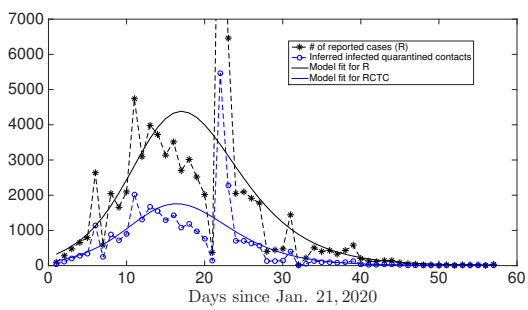

(b)

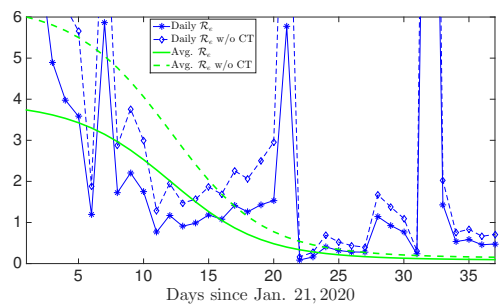

(c)

3 Reproduction Number and Outbreak Size

The reproduction number, $\mathcal{R}_e$, of the general model is derived as:

$$\mathcal{R}_e = \beta T \mathcal{S} + \beta_c T_c \mathcal{S}^c + \beta_q T_q \mathcal{S}^q, \tag{2}$$

with the current susceptibility and infection transitions of the population represented by $\mathcal{S} = (1-\phi-\xi)\,S + (1-\phi_c-\xi_c)\,\nu_c S_c + (1-\phi_q-\xi_q)\,\nu_q S_q$, $\mathcal{S}^c = \phi S + \phi_c \nu_c S_c + \phi_q \nu_q S_q$ and $\mathcal{S}^q = \xi S + \xi_c \nu_c S_c + \xi_q \nu_q S_q$. Here ν_c and ν_q are reductions in susceptibility of contact traced and social-distanced individuals, respectively, and ϕ, ϕ_c, ϕ_q and ξ, ξ_c, ξ_q are infection transition probabilities to contact traced and social-distanced states, respectively. At the outset of the

outbreak, we may assume there are no traced or social-distanced susceptible individuals, i.e. $S_c(0) = S_q(0) = 0$, and we utilize the notation $\mathcal{R}_0$, although the general formula will be utilized for (time-dependent) $\mathcal{R}_e$ calculation continuously during the outbreak.

Next we present novel theoretical results of relations between $\mathcal{R}_0$ and final outbreak size in terms of contact tracing and quarantine/social distancing. In order to obtain the results on final size, we assume that $\alpha_q = 0$ representing a sustained quarantine or social-distancing period (at least until the outbreak approaches containment) occurring at rate σ relative to infection force. In this way, final size can represent magnitude of first, second or subsequent waves where control parameters affect each outbreak size, and the required conditions for the formula may be relaxed to obtain approximate or simulated projections. Define the final proportion of susceptible individuals $U_\infty = \frac{S(\infty)}{S(0)}$ and the *final (cumulative) epidemic size* $\mathcal{C}_\infty = \int_0^\infty (I(t) + I_c(t) + I_q(t))$. In addition to $\alpha_q = 0$, we consider a few restrictions on the infection transition and susceptibility parameters, namely $\phi = \phi_c = \phi_q, \xi = \xi_c = \xi_q, \nu_c = \nu_q = \nu$, which allows for an exact formula for U_∞ and $\mathcal{C}_\infty$ dependent on the susceptibility of social distanced and contact traced individuals (ν), along with an approximation when the required conditions do not hold (see *Material and Methods* and Fig.3(b)). Furthermore, in the best case scenario where social distancing or contact tracing perfectly prevents susceptible infection ($\nu_c = \nu_q = 0$), we obtain the exact formulae:

$$\ln(U_\infty) = \mathcal{R}_0 (U_\infty - 1), \quad \mathcal{C}_\infty = S(0)\frac{1}{1+\psi}(1 - U_\infty), \tag{3}$$

where $\mathcal{R}_0 = \beta(1-\phi)TS(0)$ and $I(0) \approx 0$ in this case at the outset of the outbreak. Note that each formula can account for arbitrary initial conditions in order to quantify how $\mathcal{R}_e$ and social distancing affect outbreak size beginning at any stage (see Supplementary for formal derivations).

In the case of perfect susceptible quarantine ($\nu_q = \nu_c = 0$), we find the classical relation

between final susceptible proportion U_∞ and $\mathcal{R}_0$. This allows us to directly observe the explicit effect that the total quarantine rate ψ can have on the epidemic size $\mathcal{C}_\infty$. As opposed to contact tracing which impacts $\mathcal{R}_0$ and thus reduces final size in a nonlinear fashion, the reactive social distancing has a more simple inversely proportional relationship. For example, if we want to reduce the epidemic size by $1/2$, then the authorities should implement strict quarantine at the rate $\psi = 1$, or more expediently (because of our "force of infection" dependent responsive formulation), the rate of perfect quarantine in the population needs to exactly keep pace with the rate of new infections. The rates can be translated to time periods for more interpretability. Notice that the doubling time of cumulative incidence depends directly on the force of infection λ. Thus for the epidemic size to reduce by $1/2$, from the outbreak outset in each period of time which new infections double, the amount of individuals under perfect quarantine should also double. Likewise for $\psi = 9$, to reduce total outbreak size by factor of $1/10$, in each cumulative incidence doubling period, "perfectly quarantined" individuals should increase 10-fold. Authorities should do better than keep pace and strive for very large values of ψ, which as we will see from fitting results in Section 4, was instrumental for China rapidly curbing their epidemic.

4 Data Fitting & Efficacy of Quarantine Measures in China

We utilize data on total reported cases and quarantined contacts in mainland China published in daily reports by NHC (*9*). Although there are certain issues with the reported case data (*10*), qualitative results on how contact tracing and social distancing/lockdown measures affected outbreak size were robust when fitting raw or smoothed data (see Supplementary). We fit both our full model ((1) in Supplementary and Fig.1) and simplest model (1) simultaneously to (cumulative) reported case data and (daily number of) quarantined contacts utilizing a weighted least squares algorithm. Overall the models can fit the two datasets well with several parameter

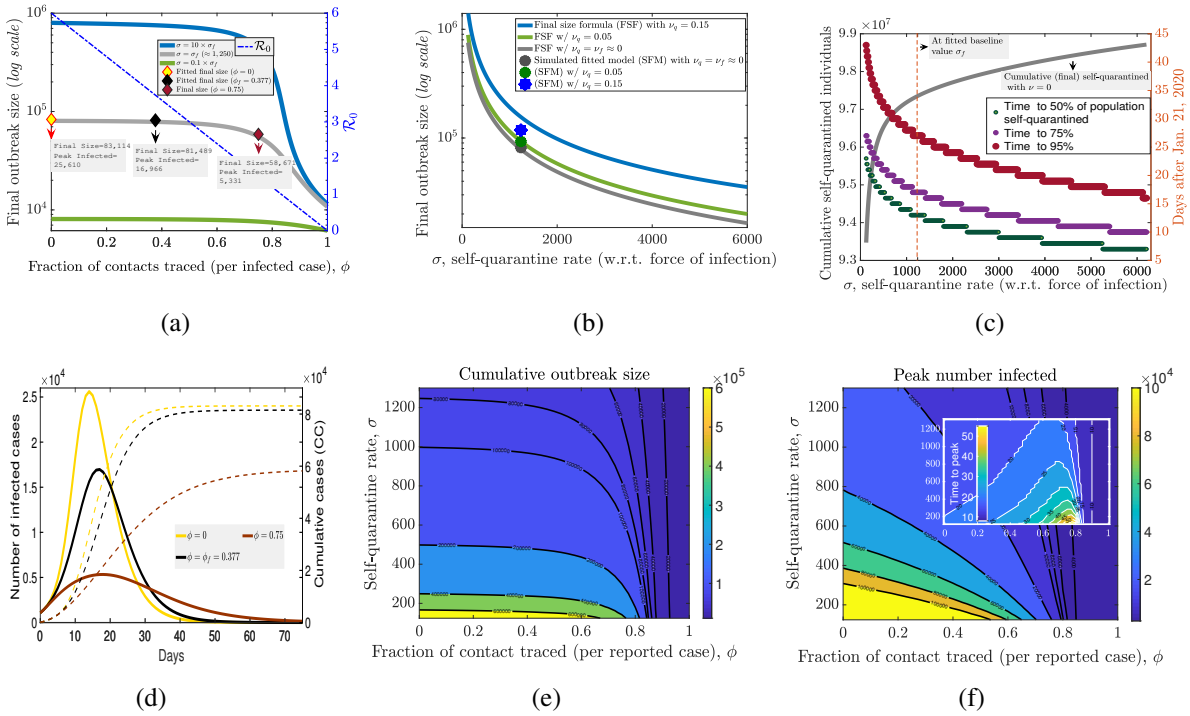

Figure 3: *Sensitivity analysis of contact tracing and self-quarantine*. All together the figures illustrate how contact tracing (ϕ) has less impact on outbreak size ($\mathcal{C}_\infty$) than self-quarantine (σ) due to underlying concavity of their nonlinear relationships derived in final size formula (3). Fitted parameter values for China show that rapidly implemented lockdowns contained the outbreak, where a delay of 2 weeks in 95% of susceptible population being self-quarantined would result in a 10-fold increase in cumulative cases. Although contact tracing had little effect (2%) on final outbreak size, it "flattened the curve", reducing peak infected by 34%. (a) Contact tracing (CT) proportion ϕ versus outbreak size $\mathcal{C}_\infty$ (nonlinear relationship) and reproduction number $\mathcal{R}_0$ (linear relationship) for 3 levels of self-quarantine (SQ) rate σ differing by order of magnitude of 10. (b) $\mathcal{C}_\infty$ as a (nonlinear) function of σ for 3 levels of SQ susceptibility reduction ν_q. (c) Total (final) self-quarantined individuals, along with time until 50%, 75%, 95% of population is self-quarantined as SQ rate σ varies. (d) Epidemic curve trajectories for 3 levels of CT proportion ϕ marked in (a). (e,f) Contour maps of outbreak size and peak infected (with time to peak inserted) depending on CT proportion ϕ and SQ rate σ.

sets. We constrained the estimations by fixing the incubation period (time to infectiousness, $\tau = 3$ days (*11*)), and infectious period (time to isolation, $T = 4.64$ days), along with a lower bound on the reduction in transmission due to contact tracing, based on a large study of cases and their contacts in Shenzhen, China (*12*).

With the above assumptions, fixing the baseline reproduction number without any control ($\mathcal{R}_{0,b} = \beta T$) produced similar results compared to when β was a fitted parameter. The value of

$\mathcal{R}_{0,b}$ chosen was 6, in line with other studies (*6,7*). Overall the extra parameters in the full model or adding unreported cases only slightly reduced error from the simplified model fit, however the additional detail in the full model allow us to vary more features of the social distancing and contact tracing interventions (see Supplementary). Although the proportion of contact traced cases varied when fitting the models under different assumptions of $\mathcal{R}_{0,b}$ or incorporating a proportion of unreported cases into model, a consistent pattern emerged on the impact of the contact tracing probability ϕ on the outbreak. Despite impacting $\mathcal{R}_0$, larger estimates of ϕ tend to correlate with larger baseline $\mathcal{R}_{0,b}$ values, which diminishes any effect on outbreak size. Based on these observations, we utilize the parameter fitting from the simplified model (1) with $\mathcal{R}_{0,b} = 6$, displayed in Fig. 2.

The best fit value of $\mathcal{R}_0$ was found to be 3.7385, CI (3.36902, 3.80467), where the estimated value of the proportion of traced contacts/reported case (ϕ) is 0.377, CI (0.349138, 0.457924). The social distancing rate (relative to force of infection) was consistently estimated to be high ($\sigma = 1240$ in displayed fit). The initial amount of infected individuals, I_0, was estimated at 778 on January 21, 2020, when the dataset begins. Note that we fit the model starting at this date, close to the time when major lockdowns began (e.g. a *cordon sanitaire* implemented in Wuhan on Jan. 23). However our force-of-infection (λ) dependent rate formulation of mass self-quarantine ($\sigma\lambda$) actually allows for a very similar epidemic trajectory when initiating the model a month earlier with one infected individual ($I_0 = 1$) and all other parameters the same as our fit starting from Jan. 21 (Supplementary Fig.S1). A full description of parameter values, along with uncertainty analysis, is presented in Supplementary.

In addition to computing $\mathcal{R}_0$ by parameter estimation of differential equation models, an alternative purely statistical approach pioneered by Wallinga and Teunisis (*13*) is to directly infer (time-dependent) $\mathcal{R}_e$ from the daily case data in combination with estimates of the serial interval (generation time) distribution. This "model-free" calculation of time varying $\mathcal{R}_e$ has

been implemented by several researchers with different serial interval distributions predicted for SARS-CoV-2 (*12, 14*). Here we incorporate both the case and quarantined contact data to infer $\mathcal{R}_e$ and efficacy of contact tracing as in a prior study of the 2014-2015 Ebola outbreak (*8*). Although missing information, in particular the amount of infected quarantined contacts, hinders our ability to directly evaluate contact tracing impact on a daily basis, we utilize the predicted relative transmission and incidence of contact traced individuals from our model fit to assess $\mathcal{R}_e$ with and without contact tracing. The results (Fig. 2) estimate the proportion of reported cases which are traced contacts and reduction of $\mathcal{R}_e$ due to contact tracing. Computation of the $\mathcal{R}_e$ from the fitted model parameters captures the general trend without the noisiness inherent in the daily case data, and indicates the strict population-wide lockdowns were the main quarantine measure (as opposed to contact tracing) which rapidly contained the outbreak in China.

Furthermore, we performed sensitivity analysis to determine the effect of the main control parameters on the final outbreak size and $\mathcal{R}_0$ (see Fig. 3). We calculated outbreak size while continuously varying contact tracing (ϕ) for distinct values of social distancing (σ) rate, utilizing our analytical expression for final size (3) (and approximation of final size for full model in Supplementary). While the inferred contact tracing level for China was not found to significantly reduce the final outbreak size, there might have been a larger effect on reducing peak infection levels by flattening the curve. In particular, by varying contact tracing proportion ϕ, observe the total reduction of 34% in peak infected size as compared to the 2% impact on cumulative outbreak size (Fig. 3(d)). In general, the time to peak infected increases with ϕ, reflecting the curve flattening, however this time period eventually decreases for sufficiently large values of ϕ as contact tracing effectively suppresses the outbreak (Supplementary Fig. S7). With sufficiently large contact tracing efficacy, outbreak size can be significantly reduced when there is less stringent lockdown (less total quarantined and more time to enact quarantine), however even in this case, some level of broader social distancing measures is almost certainly

in combination with contact tracing.

Although the social distancing rate (σ) does not affect $\mathcal{R}_0$, sensitivity analysis on the final size formula demonstrates σ has a large impact on outbreak size. There is a nonlinear relationship between social distancing and final size, which manifests in a high cost for smaller rates whereas the impact saturates for very large values of σ. The rate can be converted to time of action for social distancing to assess how delays in social distancing measures affect outbreak size (Fig. 3(c)). The estimated time for 50% of initial susceptible population of China to be social-distanced is approximately 2 weeks from Jan. 21. If this time period had been 3 weeks instead, then the total number of cases would be approximately 10 times larger. When fitting the full model, the looseness of the social distancing protocols measured by relative susceptibility of social-distanced population (ν_q) also impacts the outbreak with the outbreak size increasing at an increasing rate with respect to ν_q, although the values of ν_q are predicted to be close to zero for China and the approximation of final size becomes less accurate in the general full model with larger values of ν_q (see Fig 3(b)). Also, the estimated rate of return from social distancing (α_q) was estimated to be very small, emphasizing the strictness of the social distancing measures.

5 Quarantine Interventions for COVID-19 2nd Wave

A major question is how public health authorities should guide loosening of broad lockdown measures after initial containment of COVID-19, while optimally responding to any subsequent outbreaks induced by the relaxations. Here we analyze how the scale and rate of different reactive contact-based interventions affect 2nd wave outbreaks under two different scenarios of loosening, namely *Instantaneous Return of Several Sectors* (IRSS) or via *Gradual Return of Self-Quarantined* (GRSQ). The goal is to attain qualitative insights on the timing and allocation of control strategies for shrinking, flattening or delaying the subsequent outbreak curves. By

varying social distancing rate σ, contact tracing probability ϕ and looseness of social distancing ν under the distinct relaxation policies in our model parameterized to data from China, we observe potential consequences of different strategies.

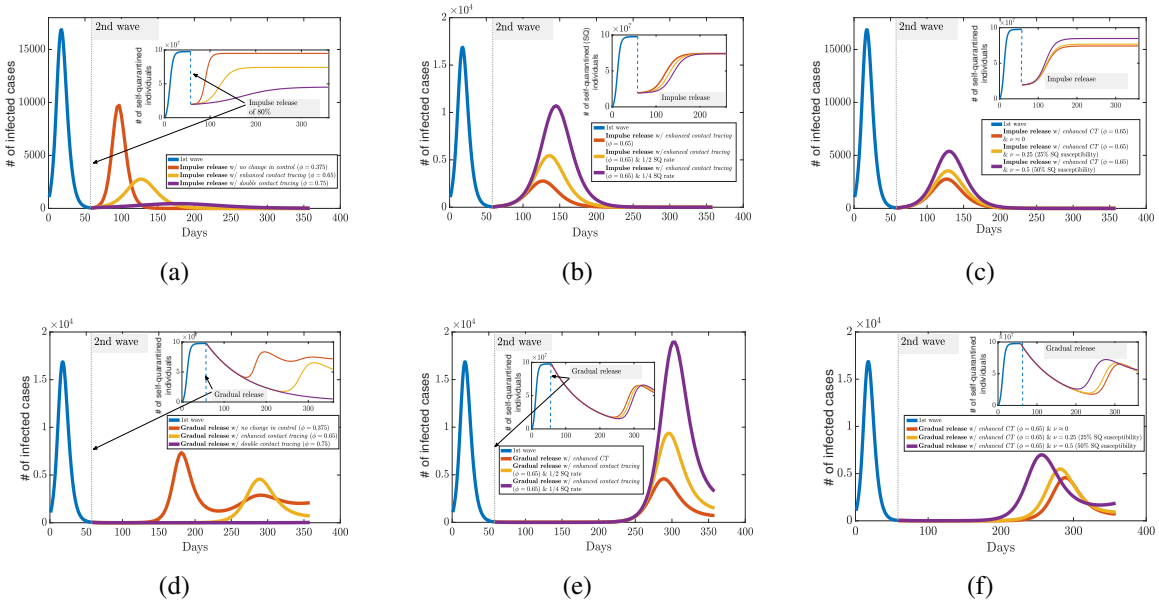

Figure 4: *Combined impact of contact tracing and responsive social distancing (self-quarantine) measures under distinct re-opening strategies.* Model simulations predict 2nd wave outbreak shape after instantaneous re-normalization of several sectors (IRSS) by releasing 80% of self-quarantined (a,b,c) versus gradual return of self-quarantined (GRSQ) to normalcy (d,e,f). Increased contact tracing levels (ϕ) can flatten or suppress (when highly effective) subsequent outbreak in (a,d). Social distancing measures responsive to new incidence shrink the outbreak size dependent on rate (σ) and looseness (ν_q) of self-quarantine in (b,e) and (c,f), respectively. In addition to the differential effects on daily infected counts of contact tracing and responsive self-quarantine (flattening versus crushing), observe the much longer delay in 2nd wave under the GRSQ re-opening policy, which can buy time for effective treatments or vaccines.

In the case of IRSS, we consider that at time t_l (when initial outbreak is close to zero), a portion, θ, of the social-distanced individuals return to susceptible compartment instantaneously; i.e. $S(t_l^+) = \theta S_q(t_l^-) + S(t_l^-)$ and $S_q(t_l^+) = (1-\theta)S_q(t_l^-)$. The terms $\theta S_q(t_l^-)$ represents the number of social-distanced individuals that "return to normalcy" at time t_l. Simulating the return of 80% of self-quarantined (social-distanced) individuals, with no change in parameters (and crucially the same reactive social distancing rate σ) we observe that the cumulative number of infected cases for the 2nd wave (outbreak size) and peak infected was 75% and 58%,

respectively, of the 1st wave. Furthermore, a similar number of individuals as during the first wave lockdown re-enter social distancing about 6 weeks after relaxation (see Fig.4(a)). When the contact tracing efforts are enhanced after lockdown (to $\phi = .65$), outbreak size and peak infected are 54% and 16%, respectively, of the 1st wave, and the curve is flattened, i.e. the peak outbreak size shrunk and the time to peak outbreak size increased. Finally if contact tracing is doubled to $\phi = 0.75$, the 2nd wave outbreak size and peak infected are 25% and 3%, respectively, of the 1st wave. In addition, the number of individuals re-entering social distancing was reduced, revealing that contact tracing can be an effective tool for managing the epidemic with a less stringent lockdown.

In the case of GRSQ strategy, after containing initial outbreak with lockdown, we increase the return to "normalcy" rate to $\alpha = 0.01$, where half the social-distanced return to normalcy in the approximate half-life time given by $t_{1/2} = \ln 2/\alpha = 72\ days$. Assuming other parameters remain constant (including the reactive SQ rate σ) the second peak, emerging with a 100 day delay, reduced to 42% of the first wave, however the number of infected individuals settle into a rather large quasi-equilibrium resulting in more cumulative cases (see Fig.4(d)). Here there is a balance of force of infection induced social distancing ($\sigma\lambda$) and reversion of individuals to their normal contact behavior (α), leading to an insufficient amount of population social distancing for reducing cases below a certain level. On the other hand, after loosening the lockdown, when the contact tracing efforts are enhanced or doubled, the peak size significantly diminished (27% or 0.3% of 1st wave), along with the number of social-distanced. Importantly, for about 6 months (or the whole year in the case of doubling ϕ), the number of infected cases stayed significantly low. This suggests that gradual release of social-distanced individuals with increasing contact tracing efforts can be utilized as a strategy to gain time until vaccination, while reinstating societal interactions in a carefully measured stepwise fashion.

Next by varying the reactive social distancing rate, we show how crucial responsive re-

implementation of social distancing measures is for reducing the second wave outbreak. Reduction in SQ rate by $1/2$ (or $1/4$), as predicted simply by the inverse proportionality in the derived final size formula (3), results in twice (or four times) more cumulative cases for the 2nd wave, and the simulations show the same relations between peak size (see Fig.4(b)). Although the number of self-quarantined individuals eventually become the same with the different SQ rates, the delay in implementing large-scale self-quarantine (in response to incidence) makes significant differences in the final (and peak) outbreak size. For the simulations presented in Fig. 4(b), a delay of just 9 days from the baseline parameter case results in twice as many infections, and a delay of 18 days induces four times the infected individuals. Compared to instantaneous release, the gradual return resulted in larger peak and total outbreak size for each SQ rate because of the increased quarantine exit rate α, but preserved the same simple proportionality relationship (see Fig.4(e)). On the other hand, gradual release still induced large time period with relatively low infected cases, which can buy time for finding an effective vaccine or treatment. Finally, varying the looseness of the quarantine (measured by uniform susceptibility and infectivity values $\nu_q = \beta_q/\beta$) from perfect quarantine to 25% (or to 50%) looseness, leads to approximately 1.3 times (or to 2 times) more total and peak infections during the outbreak. Different from the rate of SQ, the proportionality relations are nonlinear, thus a slight looseness in quarantine can still offer an effective intervention, but the cases will increase at a growing rate as the measures become less strict (see Fig.4(c),4(f)).

6 Discussion

In this study, we compare how two distinct types of contact-based control strategies, contact tracing and large-scale lockdowns/self-quarantine or social distancing, impact the characteristics of single or sequential COVID-19 outbreaks. We find that contact tracing generally is less effective in decreasing outbreak size for rapidly spreading pathogens (high baseline re-

production number $\mathcal{R}_{0,b}$), unless the tracing is very efficient. On the other hand, widespread lockdowns/social distancing interventions can lower outbreak size inversely proportional to an increase in the rate of self-quarantine. Our analysis indicates that China benefited from the heavy influence of lockdowns by rapidly containing the quickly growing COVID-19 cases, and, despite massive efforts, contact tracing was less influential in bringing down the epidemic.

Despite the difference in the targeted nature of contact tracing versus the more indiscriminate lockdown measures, we contend there is a similar reactive quality to both control strategies. Contact tracing reacts to reported cases by tracking and (to varying degrees) quarantining individuals whom have been contacted. Mass social distancing or self-quarantine reflects a natural response by both governments and individuals which intensifies as cases build, a phenomenon that has been labeled as "exponential whiplash" (*15*). These features motivate us to construct a COVID-19 model with both contact tracing (mechanistically) and self-quarantine (phenomenologically) dependent on force of infection. In contrast to another model which assumes a linear rate of self-quarantine (*6*), the nonlinear social distancing rate captures a contagion-like behavioral response to infected cases, and allows us to derive novel formulae for final outbreak size. Furthermore the model provides a good simultaneous fit to both cumulative reported cases and daily quarantined contact data from China.

An important distinction between contact tracing and lockdowns is their mode of action, namely preventing onward secondary infections by early tracking of likely infected cases in the former and large-scale depletion (or shielding) of susceptible individuals for the latter. This contrast determines how they affect the major epidemiological quantities of reproduction number and outbreak size in our "transmission-reactive" formulation. In particular, contact tracing proportionally reduces $\mathcal{R}_0$, akin to vaccination, leading to a nonlinear relationship with final outbreak size, which decreases substantially only as $\mathcal{R}_0$ approaches one. The responsive self-quarantine rate does not affect $\mathcal{R}_0$, and we derive a simple inverse proportionality with outbreak

size. Because the rate can be translated to a time of action for social distancing measures, this result analytically demonstrates the escalating impacts of delaying implementation of responsive lockdowns beyond a critical time period, which has been observed in other studies via simulation (*16, 17*). Even though similar levels of self-quarantine would eventually be reached in our model as incidence grows, the cost of delays can result in a large excess of cases.

Although we find that the extensive lockdowns and social distancing was a much larger factor in controlling COVID-19 *outbreak size* in China, our sensitivity analysis shows that contact tracing did dampen and delay *peak number of infected* despite its more limited impact on the cumulative count. In this way, contact tracing can flatten the incidence curve, easing the strain on limited hospital resources. A combination of expediently enacted contact-based interventions may be the best strategy, where effective contact tracing and responsive social distancing measures can synergistically and efficiently suppress an outbreak. However COVID-19 has proved to be a particular challenge and large-scale lockdowns have been a needed antidote for controlling outbreaks in several countries. The drastic self-quarantine orders can also reduce case numbers to a more manageable level and hopefully allow for effective contact tracing in the event of incidence occurrence after easing restrictions.

The capacity to respond to the continuing threat of COVID-19 will be vital for minimization of sequential epidemic waves. We investigated control measures under an instantaneous normalization of contact for a large portion (or several sectors) of the population versus a more gradual release of self-quarantined individuals back into social interactions. Our results show that increased contact tracing efforts can alter the second outbreak shape, either reducing and spreading out the number of infected or completely suppressing cases for highly efficient tracing. Social distancing or lockdown measures responsive to incidence can effectively compress the second peaks, with the timing being critical again. Either measure will depend upon sufficient case detection and reporting, highlighting the importance of testing. Furthermore, in-

definite or reoccurring strict lockdowns are likely to impart too high of an economic cost, and our model shows that looser restrictions and contact tracing can still reduce a second wave to manageable levels. Additionally, the strategy of gradual release of quarantined sectors can substantially delay the second wave, possibly buying time for effective treatments or vaccines to be developed.

There are factors not considered in our current study which may have played an important role in determining the COVID-19 epidemic in China. For example, we neglect a more fine-grained regional structure within China for our model and data fitting. However, a major novelty of this work was to incorporate data on the quarantined contacts, which was compiled solely for the whole of China. Obtaining provincial quarantine records may allow for simultaneous fitting of the heterogeneous spread of the virus in different regions of China. Furthermore, more detailed contact tracing data quantifying the proportion of reported cases whom were traced can allow for superior accuracy in estimating efficacy of contact tracing, which can add confidence to our conclusion that lockdowns had substantially larger influence in controlling the COVID-19 outbreak data. Nevertheless, the analytical and qualitative results here illustrate the differential effects that reactive contact tracing and lockdowns or mass self-quarantine have on outbreak shape. This knowledge and further investigation may offer insights for the public health response to COVID-19 outbreaks.

References

1. WHO, Report of the WHO-China Joint Mission on Coronavirus Disease 2019 (COVID-19), `https://www.who.int/docs/default-source/coronaviruse/who-china-joint-mission-on-covid-19-final-report.pdf` (2020).

2. M. U. Kraemer, *et al.*, *Science* **368**, 493 (2020).

3. S. Lai, *et al.*, *Nature* pp. 1–7 (2020).

4. H. Tian, *et al.*, *Science* **368**, 638 (2020).

5. J. Zhang, *et al.*, *Science* (2020).

6. B. F. Maier, D. Brockmann, *Science* **368**, 742 (2020).

7. B. Tang, *et al.*, *Available at SSRN 3537099* (2020).

8. C. Browne, H. Gulbudak, G. Webb, *Journal of theoretical biology* **384**, 33 (2015).

9. NHC, National Health Commission of the People's Republic of China, `http://en.nhc.gov.cn` (2020).

10. T. K. Tsang, *et al.*, *The Lancet Public Health* (2020).

11. X. He, *et al.*, *Nature medicine* **26**, 672 (2020).

12. Q. Bi, *et al.*, *The Lancet Infectious Diseases* (2020).

13. J. Wallinga, P. Teunis, *American Journal of epidemiology* **160**, 509 (2004).

14. L. Ferretti, *et al.*, *Science* **368** (2020).

15. *The Economist* (2020).

16. J. Dehning, *et al.*, *Science* (2020).

17. S. Pei, S. Kandula, J. Shaman, *medRxiv* (2020).

Acknowledgments

CJB, HG, and JCM are supported by a U.S. National Science Foundation RAPID grant (DMS-2028728). HG was also supported by a grant from the Simons Foundation/SFARI(638193). CJB is partially supported by an NSF grant (DMS-1815095).

Supplementary materials

Materials and Methods

Supplementary Text

Figs. S1 to S7

Tables S1 to S3

References *(1-9)*